

Irradiance-Independent Camera Color Calibration

Brian Funt,* Pouya Bastani

School of Computing Science, Simon Fraser University, Burnaby, British Columbia, Canada V5A 1S6

Received 13 February 2013; accepted 1 September 2013

Abstract: For a digital color camera to represent the colors in the environment accurately, it is necessary to calibrate the camera RGB outputs in terms of a colorimetric space such as the CIEXYZ or sRGB. Assuming that the camera response is a linear function of scene luminance, the main step in the calibration is to determine a transformation matrix \mathbf{M} mapping data from linear camera RGB to XYZ. Determining \mathbf{M} is usually done by photographing a calibrated target, often a color checker, and then performing a least-squares regression on the difference between the camera's RGB digital counts from each color checker patch and their corresponding true XYZ values. To measure accurately the XYZ coordinates for each patch, either a completely uniform lighting field is required, which can be hard to accomplish, or a measurement of the illuminant irradiance at each patch is needed. In this article, two computational methods are presented for camera color calibration that require only that the relative spectral power distribution of the illumination be constant across the color checker, while its irradiance may vary, and yet resolve for a color correction matrix that remains unaffected by any irradiance variation that may be present. © 2013 Wiley Periodicals, Inc. *Col Res Appl*, 39, 540–548, 2014; Published Online 30 October 2013 in Wiley Online Library (wileyonlinelibrary.com). DOI 10.1002/col.21849

Key words: color imaging; camera calibration; irradiance independent; intensity independent; color correction matrix

INTRODUCTION

As a general rule, color cameras need to be calibrated to produce outputs that are consistent with a standard color space, such as the CIEXYZ or sRGB.¹ This article focuses on color

calibration using a color correction matrix, as opposed to a look-up table. There are two standard methods of obtaining the training data needed for determining a color correction matrix. In the first approach, given the camera sensitivity curves, the training data can be synthesized. However, deriving the camera sensitivity functions is often time consuming and requires the use of expensive equipment such as a monochromator. The second approach is to use the actual camera outputs instead of relying on the camera's spectral sensitivity curves. A standard target, often a color checker, is photographed, and the camera output is linearized if necessary. Using the camera's linearized RGB values and the corresponding measured XYZ coordinates of each color checker patch, a color correction matrix, a mapping $\mathbf{M} : \text{RGB} \mapsto \text{XYZ}$, is computed that maps the camera's response from RGB space to XYZ. The literature on camera calibration describes many methods for obtaining such a mapping. Among these are look-up tables,² neural networks,^{3,4} white-point preserving color correction,⁵ color difference minimization,⁶ least-squares polynomial regression,² and recently root-polynomial regression.⁷ All these techniques, however, assume a priori knowledge of the XYZ coordinates of the reference color patches, data that can be difficult to obtain accurately, even in laboratory settings. One source of error in computing the ground-truth color coordinates is the assumption that the irradiance across all the color patches is uniform, when in reality it is often not uniform.

To understand the nature of errors that can arise in this process, we first note that computing the CIEXYZ coordinates of each color checker patch under a given illuminant requires knowing the reflectance spectrum of each color patch, which if unknown can be measured. In general, it is desirable to have a large number of reference patches, as this is likely to lead to a more representative final calibration. The cost of doing this is measuring the spectrum of the light reflected from each reference patch, which can be a time-consuming task (the X-Rite Digital ColorChecker SG, for instance, has 140 patches).

*Correspondence to: Brian Funt (e-mail: funt@sfu.ca)

Contract grant sponsor: Natural Sciences and Engineering Research Council of Canada.

On the other hand, it is often the case that the reflectance spectra of the patches are known, for instance, from a previous measurement. In these situations, the task of measuring the spectrum of the light reflected from each patch can be simplified to just one measurement of the spectral power distribution (SPD) of the incident illuminant, as the spectrum of the light reflected from each surface and entering the camera can be obtained by multiplying the illuminant SPD by the surface reflectance. Thus, by measuring the incident illuminant once, the necessary tristimulus coordinates can be computed easily.

However, using a single measure of the illuminant implicitly assumes uniform illumination across the calibration target. Such a uniform lighting environment is very hard to create in practice, even in a controlled environment such as a light booth. Moreover, in certain situations, such as in some robotic missions, dynamic camera calibration may be essential, and yet it may not always be safe to assume that the illumination across the robot's onboard calibration target is uniform.

In many situations where a single illuminant is present, the relative SPD of incident light often remains constant, whereas its irradiance may vary across the calibration target. If the amount of variation in the irradiance is unknown, then the true XYZ values will not correctly model the scene as captured by the camera, resulting in an incorrect color correction mapping and in turn leading to inaccurate color imaging.

To understand how nonuniform illumination affects the computation, note that a difference in irradiance on a patch results in a scaling of the associated RGB digital counts. In other words, treating RGB as a vector, its length changes but not its direction. Conventional methods of color correction, such as least-squares regression, seek to minimize the difference between transformed RGB s and XYZ s, taking into account both the direction and magnitude of RGB vectors. In this way, such techniques rely on accurate knowledge of the illuminant at each patch, for otherwise an irradiance-induced scaling in each of the RGB vectors results in an inaccurate mapping of RGB s to XYZ s.

Other more sophisticated approaches have been used in the past for performing color correction, such as that recently suggested by Finlayson *et al.*,⁷ in which root-polynomial regression is used to reduce the effect of changes in overall illuminant power or camera exposure. Although this method, unlike other higher-order regressions, is successful in compensating for changes in camera exposure, or equivalently, the illuminant power, it lacks the ability to handle any variation in irradiance across the scene.

It is thus desirable to have a color correction algorithm that relies on one measurement of the illuminant SPD, but which can reduce the effect of illuminant irradiance variation across the scene. In this article, we have presented several techniques that achieve just this goal and facilitate camera color correction that is unaffected by any nonuniformity in the irradiance.

The first method is based on minimizing the overall angular difference between camera RGB vectors and their associated XYZ vectors. This technique leads to a nonlinear optimization, which can be solved numerically to obtain the color correction transform. By considering only the angular difference between vectors, the calibration process remains unaffected by the irradiance.

The second approach to calibration discussed below is a variation on the above method that, instead of minimizing angles between target and camera RGB vectors, minimizes normalized color differences. The advantage of this technique is that, as well as accommodating nonuniform irradiance, it can easily be generalized to incorporate different measures of color difference.

As shown by Funt *et al.*⁶ in the context of display calibration, minimizing CIE ΔE differences will yield better calibration results. In the context of camera calibration, minimizing the CIE ΔE color differences between target and camera color vectors offers an advantage over calibration in CE XYZ space in that it leads to a mapping that minimizes the error in camera output directly in a perceptually uniform space. Our second approach to irradiance-independent camera calibration can also be extended to incorporate calibrations based on minimizing the error in a perceptual space. As a result, we obtained a calibration technique that, as well as minimizing the mapping error in a perceptually uniform color space, can accommodate nonuniformities in scene irradiance.

In addition, we applied our proposed calibration technique to develop a higher-order regression using root-polynomial color correction⁷ that is independent of variation in irradiance across the target as well as being independent of overall illuminant power.

Lastly, we combined the benefits of ΔE minimization, root-polynomial regression, and irradiance-independent calibration to form a higher-order regression scheme that minimizes the mean CIE ΔE error among calibration targets, while being independent of illuminant irradiance variation across the scene being photographed. Experiments showed that this combined technique provided the mapping with least average error as measured by CIEDE2000 color difference formula even under nonuniformly lit calibration scenes.

We performed experiments calibrating a camera using both captured images and ones synthesized using the camera spectral sensitivity curves. Our results show the significant degree to which irradiance variation across the target can negatively affect a traditional calibration. They also demonstrate the effectiveness of the proposed calibration technique in avoiding the problems created by nonuniform irradiance.

BACKGROUND

As mentioned above, the process of camera color calibration involves imaging a color calibration target with a camera. Formally, let $\{\mathbf{p}_i\}_{i=1}^n$ be the set of camera RGB

response vectors for n different color patches. Similarly, let $\{\mathbf{q}_i\}_{i=1}^n$ represent the set of corresponding CIEXYZ vectors computed using the measured SPD of the incident illuminant, $I(\lambda)$, the spectral reflectance function of each patch, $R_i(\lambda)$, and the CIE color matching functions, $\bar{f}(\lambda) = [\bar{x}(\lambda), \bar{y}(\lambda), \bar{z}(\lambda)]^T$:

$$\mathbf{q}_i = \int_{\lambda_{\min}}^{\lambda_{\max}} R_i(\lambda) I(\lambda) \bar{f}(\lambda) d\lambda, \quad (1)$$

where λ_{\min} and λ_{\max} are taken to be 380 and 780 nm, respectively. Conventional calibration methods find the color correction matrix, \mathbf{M} , using least-squares regression that minimizes*:

$$E_{\text{LSQ}}(\mathbf{M}) = \sum_{i=1}^n \|\mathbf{M}\mathbf{p}_i - \mathbf{q}_i\|^2. \quad (2)$$

It is well known that the best mapping minimizing Eq. (2) is given by the Moore-Penrose pseudo-inverse expression:

$$\mathbf{M} = \mathbf{Q}\mathbf{P}^T(\mathbf{P}\mathbf{P}^T)^{-1}, \quad (3)$$

where \mathbf{P} and \mathbf{Q} are the matrices whose column vectors consist of \mathbf{p}_i and \mathbf{q}_i , respectively, for $i=1, \dots, n$. As is clear from Eq. (2), both the direction and magnitude of the RGB vectors affect the regression results. Consequently, any variation in the irradiance across the calibration target that results in a corresponding scaling in the RGB s introduces error into the calibration, as the XYZ coordinates of the patches were computed assuming uniform irradiance.

We next proposed an irradiance-independent regression technique that is especially useful for camera calibration in circumstances where the scene irradiance is nonuniform.

IRRADIANCE-INDEPENDENT CALIBRATION

As scaling of the RGB color vectors affects $E_{\text{LSQ}}(\mathbf{M})$, as defined in Eq. (2), we instead seek to find a color correction matrix \mathbf{M} by minimizing a functional that does not depend on the magnitude of the color vectors. The first proposal for irradiance-independent camera calibration, which we shall refer to as angle minimization, seeks to minimize $E_{\text{AM}}(\mathbf{M})$, the sum of angle differences, θ_i , between RGB and XYZ color vectors:

$$E_{\text{AM}}(\mathbf{M}) = \sum_{i=1}^n \theta_i = \sum_{i=1}^n \cos^{-1} \left(\frac{\mathbf{M}\mathbf{p}_i \cdot \mathbf{q}_i}{\|\mathbf{M}\mathbf{p}_i\| \|\mathbf{q}_i\|} \right). \quad (4)$$

A second method, which we refer to as normalized least-distance, minimizes the sum of distances, d_i , between vectors projected onto the unit sphere as defined by $E_{\text{NLD}}(\mathbf{M})$:

$$E_{\text{NLD}}(\mathbf{M}) = \sum_{i=1}^n d_i = \sum_{i=1}^n \left\| \frac{\mathbf{M}\mathbf{p}_i}{\|\mathbf{M}\mathbf{p}_i\|} - \frac{\mathbf{q}_i}{\|\mathbf{q}_i\|} \right\|. \quad (5)$$

As can be seen, both these measures do not depend on the vector magnitudes. In fact, the relationship between $E_{\text{AM}}(\mathbf{M})$ and $E_{\text{NLD}}(\mathbf{M})$ can be seen through the relationship between d_i and θ_i . Consider the length, d , of the chord in a unit circle spanned by angle θ . For small angles, $\theta \ll 1$, using the second-degree Taylor approximation of $\cos \theta$, the relationship between them can be expressed as follows:

$$d = \sqrt{2(1 - \cos \theta)} \sim \sqrt{2 \left[1 - \left(1 - \frac{\theta^2}{2} \right) \right]} = \theta.$$

Thus, minimizing this angular difference between RGB and XYZ vectors is equivalent, to first-degree approximation in the angle, to minimizing the magnitude of the difference between the normalized vectors. Equation (4) measures the sum of angular differences between projected and target vectors, whereas Eq. (5) measures the sum of distances in L_2 norm between unit vectors.

Both these functionals lead to a nonlinear minimization problem that is solved numerically using the Nelder-Mead^{8,9} optimization method as implemented in the `fminsearch` function of MATLAB. The minimization is initialized using the least-squares solution given by Eq. (3).

Note that as the minimization is performed without regard to the overall vector magnitudes, the resulting transformation matrix \mathbf{M} is of arbitrary magnitude. In other words, an overall scaling of the transform will not alter the value of $E_{\text{AM}}(\mathbf{M})$ or $E_{\text{NLD}}(\mathbf{M})$. To define the overall magnitude of \mathbf{M} , it is rescaled by dividing it by the sum of the entries in its second row multiplied by 100. In this way, the maximum Y that can be obtained from the $RGB \rightarrow XYZ$ mapping is 100. Note that this scale factor is independent of any irradiance gradient across the calibration target as \mathbf{M} is unaffected by any irradiance variation, and thus the sum of the entries in its second row is unaffected as well. The resulting scaled color correction matrix, therefore, is unaffected by any variation in scene irradiance and is also scaled so that the maximum Y for any possible reflectance under the illuminant is 100.

NORMALIZED CIE ΔE MINIMIZATION

Although the above regression schemes remain unaffected by variations in irradiance across the calibration target, the minimization is performed in CIEXYZ space, which is not a perceptually uniform color space. Thus, the mapping \mathbf{M} obtained by minimizing $E_{\text{AM}}(\mathbf{M})$ or $E_{\text{NLD}}(\mathbf{M})$ does not necessarily lead to the perceptually most accurate mapping.

In the context of display calibration, Funt *et al.*⁶ showed that calibrating directly in a perceptually more uniform color space, such as CIELAB, reduces the calibration error as measured in terms of perceptual differences. In other words, if a calibration result is to be

*Unless otherwise stated, the L_2 norm is assumed here. For brevity, $\|\cdot\|$ will be used to denote L_2 norm $\|\cdot\|_2$.

evaluated in terms of a perceptual difference measure, such as CIELAB ΔE , then it is best to minimize the color difference directly in CIELAB in the first place. We shall refer to this calibration scheme as ΔE minimization.

To apply this technique to camera calibration (as opposed to display calibration), we need to revisit the issue of irradiance nonuniformity. Clearly, in the case of display calibration, the issue of irradiance nonuniformity does not arise. To modify the ΔE minimization approach for use in camera calibration independent of the irradiance, we first note that Eq. (4) cannot meaningfully be used to perform calibration in CIELAB space as a scaling of the XYZ vectors affects the angles between the corresponding CIELAB $L^*a^*b^*$ vectors. Nevertheless, the strategy of minimizing the normalized vector differences as in Eq. (5) can be modified to incorporate the CIELAB color difference measure:

$$E_{DE}(\mathbf{M}) = \sum_{i=1}^n \left\| \mathcal{L}_{ab}^* \left\{ \frac{\mathbf{M}\mathbf{p}_i}{\|\mathbf{M}\mathbf{p}_i\|} \right\} - \mathcal{L}_{ab}^* \left\{ \frac{\mathbf{q}_i}{\|\mathbf{q}_i\|} \right\} \right\| \quad (6)$$

$$= \sum_{i=1}^n \Delta E_{ab}^* \left(\frac{\mathbf{M}\mathbf{p}_i}{\|\mathbf{M}\mathbf{p}_i\|}, \frac{\mathbf{q}_i}{\|\mathbf{q}_i\|} \right),$$

where \mathcal{L}_{ab}^* denotes the mapping from CIEXYZ to CIELAB space, and ΔE_{ab}^* denotes the CIELAB color difference measure between two colors given in CIEXYZ space. Thus, Eq. (6) minimizes the ΔE_{ab}^* between the calibrated camera data, $\mathbf{M}\mathbf{p}_i$, and the ground-truth data, \mathbf{q}_i , after they both have been normalized to be unit vectors. In other words, the vectors $\mathbf{M}\mathbf{p}_i$ and \mathbf{q}_i are normalized in CIEXYZ space first and then mapped to CIELAB. The reference white point (X_n, Y_n, Z_n) used for the conversion to CIELAB is set to be the XYZ coordinates of the illuminant. For the D65 simulator illuminant that we used, this white point was measured to be (95.5, 100.0, 99.8).

When represented in the form given by Eq. (6), it is easy to see how $E_{DE}(\mathbf{M})$ can be generalized to any other color difference measure, ΔE :

$$E(\mathbf{M}) = \sum_{i=1}^n \Delta E \left(\frac{\mathbf{M}\mathbf{p}_i}{\|\mathbf{M}\mathbf{p}_i\|}, \frac{\mathbf{q}_i}{\|\mathbf{q}_i\|} \right). \quad (7)$$

As above, the color vectors are normalized in CIEXYZ space prior to them being converted to the color space in which the ΔE error is defined. We shall refer to this method as the normalized ΔE minimization. In particular, for the purpose of our experiments, we used the CIEDE2000 measure, ΔE_{00} , wherever ΔE is used.

NORMALIZED ROOT-POLYNOMIAL REGRESSION

Although one common method of mapping RGB values to CIEXYZ space is the 3×3 linear transform, to provide better mappings, higher-order polynomial regressions are sometimes used instead. However, as Finlayson *et al.*⁷ pointed out, using higher-order terms, such as R^2, G^2, B^2, RG, GB , and RB , in addition to the linear terms (R, G , and B) leads to the regression result becoming

dependent on any scaling of the RGB s brought about, for example, by a change in exposure. They suggested instead the idea of root-polynomial regression, where for instance, the nine terms $R, G, B, R^2, G^2, B^2, RG, GB$, and RB are replaced with the six terms $R, G, B, \sqrt{RG}, \sqrt{GB}$, and \sqrt{RB} (note that terms such as $\sqrt{R^2}$ become redundant and are dropped out). In this way, higher-order regressions can still be used without being affected by a scaling of the image RGB s.

Although the root-polynomial method successfully accounts for any overall scaling of the image RGB s, it does not account for the local scalings caused by nonuniform irradiance. This shortcoming can be resolved by combining the irradiance-independent calibration method with the root-polynomial method. Equation (5) can be adjusted to incorporate such higher-order regressions:

$$E_{NRP}(\mathbf{M}) = \sum_{i=1}^n \left\| \frac{\mathbf{M}\mathbf{p}'_i}{\|\mathbf{M}\mathbf{p}'_i\|} - \frac{\mathbf{q}_i}{\|\mathbf{q}_i\|} \right\|, \quad (8)$$

where the \mathbf{p}'_i denote camera (R, G, B) vectors extended to include the higher-order terms of root-polynomial calibration. We shall refer to this method as the normalized root-polynomial regression. We used Eq. (3) to obtain the initial guess to the numerical minimization of (8), with \mathbf{P} representing the matrix with column vectors given by \mathbf{p}'_i .

NORMALIZED ROOT-POLYNOMIAL ΔE MINIMIZATION

As the root-polynomial calibration method finds a mapping by minimizing the squared differences in CIEXYZ space, the result may not be optimal with respect to a perceptual metric such as CIELAB ΔE . The technique, however, can easily be extended to cases where the regression error is measured in a space other than that in which the regression is being performed. In particular, by using the CIEDE2000 color difference metric, we can obtain higher-order calibration methods that are not only invariant with respect to the overall intensity scaling in the image but also minimize the difference between camera and target color using a perceptual error metric. We shall refer to this calibration scheme as root-polynomial ΔE minimization.

In addition, to remove the effects of relative variation in the illuminant irradiance across the scene, we proposed combining the root-polynomial ΔE minimization technique with the normalized ΔE minimization using Eq. (7) as a way of obtaining a calibration that has the benefits of root-polynomial regression, is invariant to irradiance variations, and is optimal in terms of a perceptual error metric. This calibration method minimizes:

$$E(\mathbf{M}) = \sum_{i=1}^n \Delta E \left(\frac{\mathbf{M}\mathbf{a}'_i}{\|\mathbf{M}\mathbf{a}'_i\|}, \frac{\mathbf{q}_i}{\|\mathbf{q}_i\|} \right). \quad (9)$$

We shall refer to this technique as normalized root-polynomial ΔE minimization.

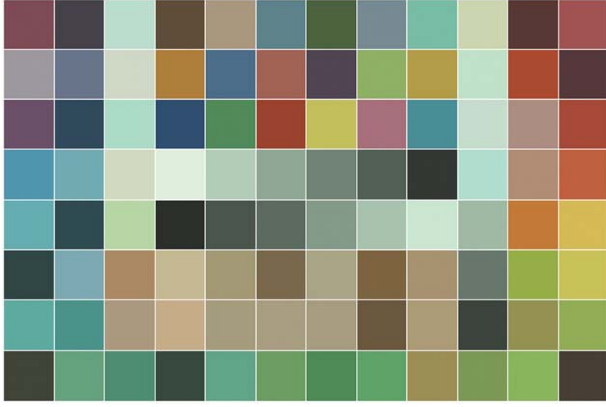


FIG. 1. Plot of the colors of the interior patches of the X-Rite Digital ColorChecker SG captured in the light booth by the camera.

EXPERIMENTS USING CAPTURED IMAGES

To evaluate the effectiveness of the proposed irradiance-independent calibration, we calibrated a Point Grey Research, Inc., Grasshopper GRAS-20S4C model camera using the X-Rite Digital ColorChecker SG. An image of the color checker is taken inside the Macbeth Judge II light booth under the D65 light source simulator. Several RAW-format linear images of the color checker are captured and averaged to minimize noise. The achromatic patches around the border are excluded, leaving 96 interior patches. The RGB values across each patch are averaged to reduce noise, resulting in the set of colors shown in Fig. 1. As the signal-to-noise ratio is low for the dark patches, dark patches for which $X+Y+Z < 25$ were removed from this set (see below for calculation of XYZ coordinates). Ten patches were removed leaving $n=86$ color vectors $\{\tilde{p}_i\}_{i=1}^n$ to be used in the calibration process.

As the light source is located at the top of the light booth, there is unavoidably some variation in the illuminant irradiance across the color checker that was placed against the back wall of the light booth. Although this nonuniformity is barely visible in the RAW image of the color checker, it can be measured by taking a picture of the gray back wall with the color checker removed. Sampling the RGB values at the same locations as the patches of the color checker yields the background irradiance variation map[†] (Fig. 2). The ratio of maximum to minimum $R+G+B$ across the color checker was 1.5.

Based on the measured background irradiance map, we scaled the (R, G, B) values of each patch from the image of the color checker to simulate uniform illumination. Thus, we have an original image captured under nonuniform lighting and one that is corrected for the irradiance variation and therefore represents the image that would have been captured under uniform lighting. The set of

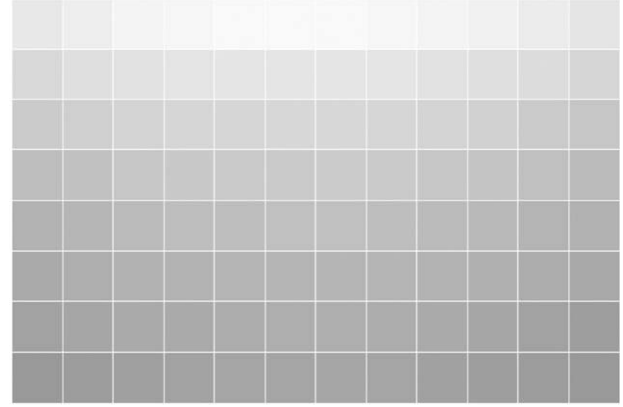


FIG. 2. Plot illustrating the illuminant irradiance variation across the color checker, obtained by photographing the back wall.

these colors, represented by vectors $\{p_i\}_{i=1}^n$, will be used as the ground-truth data.

We used Eq. (1) to compute the set of “true” tristimulus values of the color patches, $\{q_i\}_{i=1}^n$. The SPD of the light booth illuminant, $I(\lambda)$, is measured using a PR-650 SpectraScan Colorimeter. The reflectance spectrum of each patch, $\{R_i(\lambda)\}_{i=1}^n$, was measured in a previous experiment. Note that in using the same SPD, $I(\lambda)$, to obtain the XYZ coordinates of the patches, we are implicitly assuming that the illuminant irradiance is constant across the calibration target. When the reflectance spectra of the color patches are known, this simplifying assumption eliminates the need to measure the spectrum reflected from each patch. However, in the presence of irradiance nonuniformity across the color checker being photographed, as in Fig. 2, the camera calibration could be affected by the irradiance nonuniformity depending on the method used.

We performed two sets of tests to compare the performance under nonuniform lighting of the various calibration methods mentioned in this article. The four techniques that are susceptible to variation in illuminant irradiance are as follows:

1. Least-squares minimization
2. ΔE_{00} minimization
3. Root-polynomial minimization
4. Root-polynomial ΔE_{00} minimization

We compared the results from the above techniques to the following irradiance-independent calibration methods:

5. Angle minimization
6. Normalized least-distance minimization
7. Normalized ΔE_{00} minimization
8. Normalized root-polynomial minimization
9. Normalized root-polynomial ΔE_{00} minimization

To evaluate the extent to which an irradiance variation across the color checker affects the calibration results, we first calibrated the camera using the raw camera RGB s of the color checker, $\{\tilde{p}_i\}_{i=1}^n$, to obtain the color correction

[†]The image displayed is gamma adjusted in order to make visible the variation in intensity, which would otherwise be hard to see. The original data is linear.

TABLE I. Relative difference in terms of Frobenius matrix norm between color correction matrices $\tilde{\mathbf{M}}$ and \mathbf{M} .

	$\ \mathbf{M}-\tilde{\mathbf{M}}\ _F/\ \mathbf{M}\ _F$
Least squares	0.1400
ΔE_{00} minimization	0.0799
Root-polynomial	0.4357
Root-polynomial ΔE_{00} minimization	0.4378
Angle minimization	0.0000
Normalized least distance	0.0000
Normalized ΔE_{00} minimization	0.0000
Normalized root-polynomial	0.0000
Normalized root-polynomial ΔE_{00} minimization	0.0000

Zero indicates that $\mathbf{M}=\tilde{\mathbf{M}}$, as is expected for irradiance-independent calibration.

matrix $\tilde{\mathbf{M}}$. This calibration is affected by any irradiance nonuniformity across the color checker. For each method, we also used the irradiance-adjusted camera RGB s from the ground-truth image, $\{\mathbf{p}_i\}_{i=1}^n$, to obtain a corresponding ground-truth transform \mathbf{M} . For methods 1, 2, 5, 6, and 7, the color correction matrices $\tilde{\mathbf{M}}$ and \mathbf{M} are 3×3 matrices, whereas for the remaining cases involving root-polynomial regression, they are 3×6 matrices mapping $(R, G, B, \sqrt{RG}, \sqrt{GB}, \sqrt{RB})$ to (X, Y, Z) .

One method of evaluating the effect of illuminant irradiance variation on the camera calibration result is to compute the relative difference between color correction matrices $\tilde{\mathbf{M}}$ and \mathbf{M} , for which the Frobenius matrix norm[‡] $\|\cdot\|_F$ provides one measure as follows:

$$\text{relative difference} = \frac{\|\mathbf{M}-\tilde{\mathbf{M}}\|_F}{\|\mathbf{M}\|_F}. \quad (10)$$

In other words, the relative difference between $\tilde{\mathbf{M}}$ and \mathbf{M} is a measure of the degree to which the irradiance variation affects the calibration. As shown in Table I, the relative error in the transform obtained using the nonuniformly lit image can be quite significant for the calibration methods requiring uniform lighting. On the other hand, the zeros in the last five rows of the table indicate that the irradiance-independent calibration methods are completely unaffected by any nonuniformity in the scene irradiance. That they are unaffected by the irradiance follows from the fact that for any arbitrary non-zero scaling, α_i , of the RGB \mathbf{p}_i of the i th color patch, that is, if $\tilde{\mathbf{p}}_i = \alpha_i \mathbf{p}_i$, we have

$$\frac{\mathbf{M}\tilde{\mathbf{p}}_i}{\|\mathbf{M}\tilde{\mathbf{p}}_i\|} = \frac{\mathbf{M}(\alpha_i \mathbf{p}_i)}{\|\mathbf{M}(\alpha_i \mathbf{p}_i)\|} = \frac{\alpha_i \mathbf{M}\mathbf{p}_i}{\|\alpha_i \mathbf{M}\mathbf{p}_i\|} = \frac{\alpha_i \mathbf{M}\mathbf{p}_i}{\alpha_i \|\mathbf{M}\mathbf{p}_i\|} = \frac{\mathbf{M}\mathbf{p}_i}{\|\mathbf{M}\mathbf{p}_i\|}. \quad (11)$$

As a result, the generalized minimization problems for \mathbf{M} and $\tilde{\mathbf{M}}$ as given by Eq. (7) become equivalent:

[‡]The Frobenius norm of a matrix is given by the square root of the sum of the squares of the matrix elements.

TABLE II. ΔE_{00} statistics for multiple calibration methods.

	Mean ΔE_{00}	Median ΔE_{00}	Maximum ΔE_{00}
Least squares	3.46	2.70	16.77
ΔE_{00} minimization	2.88	2.54	9.44
Root-polynomial	2.47	2.05	8.78
Root-polynomial ΔE_{00} minimization	2.55	2.28	8.12
Angle minimization	2.80	2.29	9.44
Normalized least distance	2.78	2.31	9.45
Normalized ΔE_{00} minimization	2.90	2.42	8.89
Normalized root-polynomial	3.42	3.05	12.43
Normalized root-polynomial ΔE_{00} minimization	3.36	3.03	10.16

Errors were obtained when the color correction matrices are calculated using the raw image (with irradiance gradient) as input.

$$E(\tilde{\mathbf{M}}) = \sum_{i=1}^n \Delta E \left(\frac{\mathbf{M}\tilde{\mathbf{p}}_i}{\|\mathbf{M}\tilde{\mathbf{p}}_i\|}, \frac{\mathbf{q}_i}{\|\mathbf{q}_i\|} \right) \quad (12)$$

$$= \sum_{i=1}^n \Delta E \left(\frac{\mathbf{M}\mathbf{p}_i}{\|\mathbf{M}\mathbf{p}_i\|}, \frac{\mathbf{q}_i}{\|\mathbf{q}_i\|} \right) = E(\mathbf{M}),$$

where, as stated earlier, all color vectors, $\mathbf{M}\mathbf{p}_i$, $\mathbf{M}\tilde{\mathbf{p}}_i$, and \mathbf{q}_i , are first normalized and then converted to the color space required for the color difference metric ΔE . Thus, with or without a nonuniformity of the irradiance, the irradiance-independent methods determine the same color correction matrix, that is, $\mathbf{M}=\tilde{\mathbf{M}}$ or $\|\mathbf{M}-\tilde{\mathbf{M}}\|_F/\|\mathbf{M}\|_F=0$.

The results in Table I measure the differences in the color correction matrices when the calibration assumes uniform irradiance, but the irradiance is in fact nonuniform. It is also important to determine how much these differences affect the mapping of colors from camera RGB to CIEXYZ space. Hence, we compute the residual error in the calibration. As the XYZ coordinates of the patches were computed assuming uniform irradiance, to compute the residual error, we need to use the ground-truth image (i.e., having any irradiance gradient removed) as input as well. For each method, we apply both \mathbf{M} and $\tilde{\mathbf{M}}$ to the ground-truth image to obtain two sets of mapped XYZ s, $\{\mathbf{M}\mathbf{p}_i\}_{i=1}^n$ and $\{\tilde{\mathbf{M}}\mathbf{p}_i\}_{i=1}^n$. We then compute the ΔE_{00} color difference between the tristimulus values, $\{\mathbf{q}_i\}_{i=1}^n$, of the ground-truth image and the result of applying the two matrices to the ground-truth image, $\{\mathbf{M}\mathbf{p}_i\}_{i=1}^n$ and $\{\tilde{\mathbf{M}}\mathbf{p}_i\}_{i=1}^n$. In other words, we map the RGB s, \mathbf{p}_i (without any further adjustment of their magnitudes) from the ground-truth image to CIEXYZ using both \mathbf{M} and $\tilde{\mathbf{M}}$ and then determine the distance to the target XYZ s, \mathbf{q}_i , in CIELAB space using the following formulae:

$$D_i(\mathbf{M}) = \Delta E_{00}(\mathbf{M}\mathbf{p}_i, \mathbf{q}_i) \text{ and } D_i(\tilde{\mathbf{M}}) = \Delta E_{00}(\tilde{\mathbf{M}}\mathbf{p}_i, \mathbf{q}_i), \quad (13)$$

where i is the index of the i th patch.

Table II shows the mean, median, and maximum of $\{D_i(\tilde{\mathbf{M}})\}_{i=1}^n$ computed across all patches for each calibration method. Similarly, Table III shows the mean, median, and maximum of $\{D_i(\mathbf{M})\}_{i=1}^n$ when the camera is calibrated on the ground-truth (no gradient) image and

TABLE III. ΔE_{00} statistics for multiple calibration methods.

	Mean ΔE_{00}	Median ΔE_{00}	Maximum ΔE_{00}
Least squares	3.03	2.45	11.43
ΔE_{00} minimization	2.69	2.18	9.33
Root-polynomial	2.24	1.78	7.85
Root-polynomial ΔE_{00} minimization	2.10	1.53	8.06
Angle minimization	2.80	2.29	9.44
Normalized least distance	2.78	2.31	9.45
Normalized ΔE_{00} minimization	2.90	2.42	8.89
Normalized root-polynomial	3.42	3.05	12.43
Normalized root-polynomial ΔE_{00} minimization	3.36	3.03	10.16

The color correction matrix is obtained by calibrating on the ground-truth (irradiance-adjusted) image and is tested on the same image.

the resulting transform is applied to the same image. The errors for the proposed methods are the same in both cases; however, errors increase for the traditional methods when the irradiance gradient is present. The tables also show that when the irradiance gradient is small or non-existent, the irradiance-dependent methods can result in a more accurate calibration.

Overall, the above results demonstrate the effectiveness of our proposed calibration techniques in accommodating any irradiance variation across the calibration target. Moreover, the methods offer accurate mapping of camera *RGB* to CIEXYZ space.

EXPERIMENTS USING SYNTHESIZED IMAGES

To evaluate the performance of the various calibration methods under more controlled conditions, we performed additional tests using synthetic image data. Having measured the SPD of light booth’s simulated D65 source and obtained the camera’s spectral sensitivity curves, we synthesized the *RGB* values of the 96 interior patches of the X-Rite Digital ColorChecker SG under uniform lighting

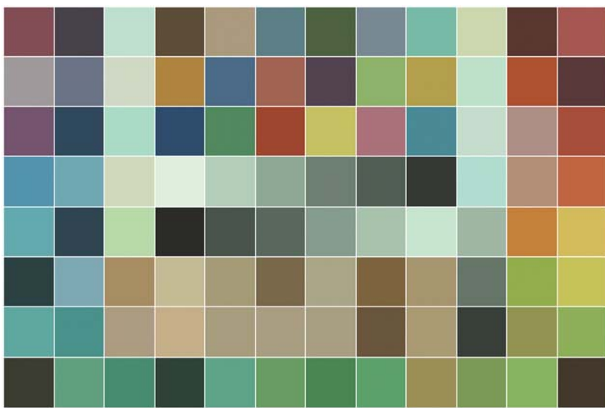


FIG. 3. Plot of the colors of the interior patches of the X-Rite Digital ColorChecker SG, synthesized under uniform lighting using the camera’s sensitivity curves.

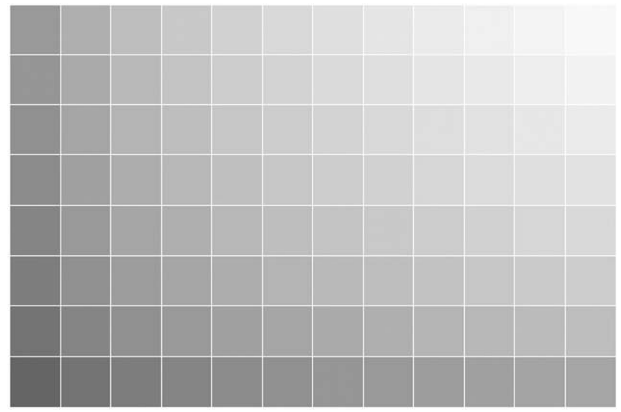


FIG. 4. Synthesized image of the irradiance variation. The grayscale value represented by each square is multiplied by the synthesized *RGB* of the corresponding patch.

(Fig. 3). For consistency with the real-image experiments, we excluded the same 10 dark patches as before. The remaining set of $n=86$ color vectors, $\{\mathbf{p}_i\}_{i=1}^n$, form the ground-truth *RGB* values without irradiance variation. The *XYZ* coordinates of the patches, $\{\mathbf{q}_i\}_{i=1}^n$, are the same as before. In the previous experiments, we reduced the effect of irradiance variation to obtain the ground-truth image, whereas in these experiments, we deliberately introduced some variations in the original synthesized camera output by scaling the *RGB* values of the i th patch by α_i to obtain $\tilde{\mathbf{p}}_i = \alpha_i \mathbf{p}_i$. The synthesized background irradiance variation is shown in Fig. 4. The ratio of the largest intensity value (top-right corner) to the smallest (bottom-left corner) is $2.5 = \max\{\alpha_i\}$. The set of “true” tristimulus values of the color patches, $\{\mathbf{q}_i\}_{i=1}^n$, is the same as in the previous section.

As in the case of the real-image experiments, the color correction matrices \mathbf{M} and $\tilde{\mathbf{M}}$ are computed using synthesized camera *RGB*s, $\{\mathbf{p}_i\}_{i=1}^n$ and $\{\tilde{\mathbf{p}}_i\}_{i=1}^n$, respectively. The degree to which the calibration is affected by the synthesized irradiance variation is measured, as before, by computing the relative error in $\tilde{\mathbf{M}}$ using Eq. (9). The results in Table IV demonstrate that the error in the color

TABLE IV. Relative difference in terms of Frobenius matrix norm between color correction matrices \mathbf{M} and $\tilde{\mathbf{M}}$, computed using the unadjusted and adjusted synthetic images, respectively.

	$\ \mathbf{M} - \tilde{\mathbf{M}}\ _F / \ \mathbf{M}\ _F$
Least squares	0.2611
ΔE_{00} minimization	0.3494
Root-polynomial	0.7813
Root-polynomial ΔE_{00} minimization	0.7463
Angle minimization	0.0000
Normalized least distance	0.0000
Normalized ΔE_{00} minimization	0.0000
Normalized root-polynomial	0.0000
Normalized root-polynomial ΔE_{00} minimization	0.0000

Zero indicates that $\mathbf{M} = \tilde{\mathbf{M}}$, as is expected for irradiance-independent calibration.

TABLE V. ΔE_{00} statistics for the methods when calibration is based on the synthesized image of the color checker under nonuniform lighting and is tested on the ground-truth image.

	Mean ΔE_{00}	Median ΔE_{00}	Maximum ΔE_{00}
Least squares	4.93	5.06	9.87
ΔE_{00} minimization	6.50	6.92	10.15
Root-polynomial	5.11	5.44	7.95
Root-polynomial ΔE_{00} minimization	6.85	7.69	11.22
Angle minimization	3.22	2.90	7.58
Normalized least distance	3.22	2.90	7.58
Normalized ΔE_{00} minimization	3.14	2.76	8.17
Normalized root-polynomial	3.36	3.05	8.78
Normalized root-polynomial ΔE_{00} minimization	2.93	2.61	7.53

correction matrix can be large if the irradiance variation is not accounted for, especially for the methods involving root-polynomial regression.

To evaluate the effect of the irradiance variation on the calibration result, we measured the residual error in the calibration in the same way as described above for the captured images. In particular, we computed $D_i(\mathbf{M})$ and $D_i(\tilde{\mathbf{M}})$ using Eq. (13). Table V shows the mean, median, and maximum of the CIEDE2000 differences $\{D_i(\tilde{\mathbf{M}})\}_{i=1}^n$ between $\tilde{\mathbf{M}}\mathbf{p}_i$ and \mathbf{q}_i , when the calibration is performed using $\{\tilde{\mathbf{p}}_i\}_{i=1}^n$ and then tested using the ground-truth values, $\{\mathbf{p}_i\}_{i=1}^n$. Table VI shows the same quantities for $\{D_i(\mathbf{M})\}_{i=1}^n$, taken between $\mathbf{M}\mathbf{p}_i$ and \mathbf{q}_i when the camera is calibrated using the ground-truth (no gradient) synthesized *RGBs*, $\{\mathbf{p}_i\}_{i=1}^n$ and then tested on them as well.

Note that as discussed previously, for the irradiance-independent methods, $D_i(\mathbf{M})=D_i(\tilde{\mathbf{M}})$ for all i . This is the reason that the numbers in the last five rows of Tables V and VI are precisely the same, irrespective of the magnitude of the irradiance gradient. In comparison, for the irradiance-dependent calibration methods, the errors increase when the calibration target is not lit uniformly. However, as Table VI shows, if the illuminant irradiance is perfectly uniform, the irradiance-dependent methods can lead to slightly more accurate calibration. When there is no gradient present, the irradiance-independent methods are at a slight disadvantage because they implicitly assume that all patches have the same overall intensity and so discard all relative irradiance information.

The synthetic calibrations further demonstrate the inaccuracies that can result when calibrating a camera on a non-uniformly lit image of a color checker. In addition, they show that the irradiance-independent calibration techniques completely account for variations in irradiance so that the resulting color correction matrix is unaffected by it.

DISCUSSION AND CONCLUSION

We propose a color calibration technique that does not require uniform irradiance across the calibration target.

TABLE VI. ΔE_{00} statistics for the methods when calibration is based on the synthesized image of the color checker under uniform lighting and is tested on the same ground-truth image.

	Mean ΔE_{00}	Median ΔE_{00}	Maximum ΔE_{00}
Least squares	2.98	2.62	7.20
ΔE_{00} minimization	2.65	2.10	7.18
Root-polynomial	2.37	1.99	6.22
Root-polynomial ΔE_{00} minimization	2.17	1.63	6.20
Angle minimization	3.22	2.90	7.58
Normalized least distance	3.22	2.90	7.58
Normalized ΔE_{00} minimization	3.14	2.76	8.17
Normalized root-polynomial	3.36	3.05	8.78
Normalized root-polynomial ΔE_{00} minimization	2.93	2.61	7.53

Although conventional methods, such as least-squares regression, take into account both the magnitude and direction of color vectors in mapping uncalibrated camera *RGB* output to *XYZ* coordinates, our method eliminates the dependence on the scene irradiance and the resulting image color intensities by considering only vector directions.

Two methods of accounting for variations in irradiance were suggested: angle minimization and normalized least-distance. Although these two methods are very similar, the second method is more easily combined with other calibration techniques, such as root-polynomial regression and ΔE minimization. Such combined methods exhibit the irradiance independence of our formulation while maintaining the other methods' original advantages. Specifically, root-polynomial regression solves the exposure problem plaguing polynomial regression, and normalized root-polynomial regression makes the root-polynomial regression independent of irradiance variations as well. Furthermore, combining normalized root-polynomial regression with ΔE minimization results in calibration based on a perceptual metric.

Testing using both real and synthetic data shows the effectiveness of the proposed irradiance-independent class of methods. In addition, the tests show that unaccounted-for irradiance variation can significantly affect the resulting color correction matrix as derived by traditional methods, with a concomitant reduction in the accuracy of the resulting colors. The proposed irradiance-independent calibration methods were found to be only slightly less accurate than traditional methods in situations where the irradiance can be controlled to be perfectly spatially constant. If the irradiance is easily controlled then it may be preferable to use traditional methods. However, there are many circumstances where this may not be possible as, for example, when a photographer includes a color checker in an image as a way of ensuring accurate color. The proposed methods offer the advantage of being completely unaffected by any irradiance gradient, and thus these methods deliver precisely the same calibration accuracy whether or not the irradiance varies.

ACKNOWLEDGMENT

The authors thank the anonymous reviewers for their helpful comments.

1. Wyszecki G, Stiles W. Color Science: Concepts and Methods, Quantitative Data and Formula, 2nd edition. New York: Wiley; 1982.
2. Hung P. Colorimetric calibration in electronic imaging devices using a look-up-table model and interpolations. *J Electron Imaging* 1993;2:53–61.
3. Hong G, Luo MR, Rhodes PA. A study of digital camera colorimetric characterization based on polynomial modeling. *Color Res Appl* 2001; 26:76–84.
4. Cheung T, Westland S. Color camera characterization using artificial neural networks. *Color Res Appl* 2001;26:76–84.
5. Finlayson G, Drew M. White-Point Preserving Color Correction. In Proceedings of the IS&T Fifth Color Imaging Conference. Society for Imaging Science and Technology, Springfield VA: IS&T, 1997. p 258–261.
6. Funt B, Ghaffari R, Bastani B. Optimal linear *RGB*-to-*XYZ* mapping for color display calibration. In Proceedings of the 12th Color Imaging Color Science, Systems and Applications, Scottsdale, AZ, November: Color Science, Systems and Applications, Society for Imaging Science and Technology, Springfield VA: IS&T, 2004. p. 223–227.
7. Finlayson G, Mackiewicz M, Hurlbert A. Root polynomial color correction. In Proceedings of the IS&T/SID 19th Color Imaging Conference. Society for Imaging Science and Technology, Springfield VA: IS&T, 2011. p 115–119.
8. Nelder JA, Mead R. A simplex method for function minimization. *Comput J* 1965;7:308–313.
9. Lagarias JC, Reeds JA, Wright MH, Wright PE. Convergence properties of the Nelder–Mead simplex method in low dimensions. *SIAM J Optimization* 1998;9:112–147.

COMMUNICATIONS AND COMMENTS

(Continued from page 636)

I will leave the evaluation of D_{ab}^* as a correlate of perceived depth of shade to others. Perhaps I will be prescient rather than naïve?

ROY S. BERN^{S*}
Munsell Color Science Laboratory

Program of Color Science
Rochester Institute of Technology
54 Lomb Memorial Drive, Rochester, NY 14623-5604

Published Online 30 August 2014 in Wiley Online Library (wileyonlinelibrary.com). DOI 10.1002/col.21918

*Correspondence to: Roy S. Berns
(e-mail: berns@cis.rit.edu)